J. Fluid Mech. (2008), *vol.* 605, *pp.* 355–366.
doi:10.1017/S0022112008001511 Printed in the United Kingdom

A physical mechanism of the energy cascade in homogeneous isotropic turbulence

SUSUMU GOTO

Department of Mechanical Engineering and Science, Kyoto University,
Yoshida-Honmachi, Sakyo, Kyoto 606-8501, Japan

(Received 7 November 2007 and in revised form 13 March 2008)

In order to investigate the physical mechanism of the energy cascade in homogeneous isotropic turbulence, the internal energy and its transfer rate are defined as a function of scale, space and time. Direct numerical simulation of turbulence at a moderate Reynolds number verifies that the energy cascade can be caused by the successive creation of smaller-scale tubular vortices in the larger-scale straining regions existing between pairs of larger-scale tubular vortices. Movies are available with the online version of the paper.

1. Introduction

Many theories of turbulence are based on the similarity hypothesis of Kolmogorov (1941): small-scale turbulent motions are statistically independent of the largest-scale flow structures, and therefore small-scale statistics become universal irrespective of the mechanism sustaining the turbulence. It is well known (see § 5 of Frisch 1995) that laboratory experiments, field measurements and direct numerical simulations (DNS) support, for example, the universality of the energy spectrum for large wavenumbers.

The similarity hypothesis relies on the energy cascade picture, which is described well by the famous verse on page 66 of Richardson (1922): 'big whirls have little whirls that feed on their velocity, and little whirls have lesser whirls and so on to viscosity'. In other words the energy supplied to large scales transfers to smaller and smaller scales until it is dissipated at the Kolmogorov scale η, below which the dissipative effect dominates the nonlinear energy transfer. It is fundamental that the energy cascades successively from larger to smaller scales, and that the conditions at the largest scale are forgotten through the local-in-scale energy transfer. It has been shown numerically (Domaradzki & Rogallo 1990, for example) and theoretically (Kraichnan 1971) that non-local interactions of the Fourier modes of velocity produce relatively local energy transfer in the Fourier space. A recent development on the localness of the energy cascade is given by Eyink (2005).

The question then arises: what happens in the physical space? Although a number of authors have referred to the physical-space energy cascade (see e.g. Hunt *et al.* 2001; Tsinober 2001; Davidson 2004), proposed scenarios seem not to be conclusive because of the lack of numerical or experimental verifications. Hence, in this article we numerically examine energy transfer in the physical space, and show that the energy cascade can be caused by the stretching of smaller-scale vortices in larger-scale strains existing between vortex pairs.

Although one of the strategies to attack this problem is wavelet analysis (see Farge 1992 for its basic idea), here we adopt a much simpler method with which we address the following two points. One is that the cascading quantity is the energy, i.e. half the

squared velocity, which is *not* a Galilean invariant. However, the cascade process itself must be independent of the frame of reference. Therefore, in our method, the whole system is divided into sub-domains, and we decompose the total energy of the fluid particles in each sub-domain into the translational energy and its internal counterpart. Note that the internal energy thus defined is a Galilean invariant. The other is that, as emphasised by Meneveau & Lund (1994) and Pumir, Shraiman & Chertkov (2001), there is an important difficulty in describing the dynamics such as the energy cascade of developed turbulence from the Eulerian viewpoint. This is a difficulty encountered by two-point closures (Kraichnan 1965), and it is likely to be related to the non-local interactions between the Fourier modes of the Eulerian velocity being conspicuous (Domaradzki & Rogallo 1990; Yeung & Brasseur 1991; Ohkitani & Kida 1992, and others) though the energy transfers locally in scale. In other words, the sweeping in developed turbulence is too strong to describe its inherent dynamics at a fixed point in the laboratory frame. Therefore, in our method, the transfer rate of the internal energy is defined in the frame moving with the sweeping velocity (i.e. from a Lagrangian viewpoint).

2. A scenario of the energy cascade

The numerical results shown in the next section suggest the following as a possible scenario of the energy cascade in homogeneous isotropic turbulence. The energy supplied to a large scale $\mathscr{L}$ is possessed by tubular vortices with radii of $O(\mathscr{L})$. When two of these vortices meet, a strong strain field of this scale is created between the pair. Then, smaller-scale (say, $\mathscr{L}'$) tubular vortices can be stretched and created by this large-scale strain. In other words, the energy transfers from $\mathscr{L}$ to the smaller scale $\mathscr{L}'$ due to the stretching of smaller-scale vortices within the large-scale strain. Then, the energy at scale $\mathscr{L}'$ is possessed by the tubular vortices with radii of $O(\mathscr{L}')$. Subsequently, when two of these vortices meet smaller-scale (say, $\mathscr{L}''$) tubular vortices are created in the strong strain field of scale $\mathscr{L}'$ between the pair. Through this process, part of the energy inside the tubular vortices of size $\mathscr{L}'$ transfers to the tubular vortices of size $\mathscr{L}''$. After several steps of such vortex stretching processes, the energy transfers to tubular vortices (so-called *worms*; see Jiménez *et al.* 1993 and references therein) with radii of $O(\eta)$, and it is dissipated in strain-dominant regions around these smallest-scale tubular vortices. Note that the final energy dissipation stage at η is widely recognised (see e.g. Kerr 1985; Brachet 1991; Vincent & Meneguzzi 1994; Kida & Miura 2000), and the cascade process may be regarded as its manifestation in the inertial-range scales between η and $\mathscr{L}$.

The above scenario is not a completely new view and is shared, to some extent, by many turbulence researchers (for example, Melander & Hussain 1993; Davidson 2004). It is also consistent with the inverse energy cascade in two-dimensional turbulence, where no vortex stretching takes place. Chen *et al.* (2006) suggested, based on a careful analysis of the data of laboratory and numerical experiments, that the thinning and weakening (instead of the stretching and strengthening in three-dimensional turbulence) of smaller-scale vortices by larger-scale strains lead to the inverse energy cascade.

3. Numerical verification

The turbulent fields analysed below are simulated by a standard dealiased Fourier spectral method. The fluid is incompressible and confined in a periodic box with 512^3

grid points. By an artificial force at large scales, statistically stationary turbulence at a moderate Reynolds number (Taylor-length-based Reynolds number is $R_\lambda \approx 187$, data A) is sustained. (Note that the magnitudes of the Fourier components of vorticity in the wavenumber region $k < \sqrt{8}$, which corresponds to the scales larger than about 410η, are fixed. Since their phases evolve, the largest-scale structures are not steady.) We also analyse in § 3.3 the artificial velocity field (data B) which is smoothed by low-pass filtering the Fourier modes at a cut-off wavenumber, $k_c = 16$. The aim of this analysis (data B) is to consider the generation mechanism of smaller-scale structures.

The numerical grid width Δ is about 2.3η. The size of the periodic cube is $L_0 \approx 7\mathscr{L} \approx 1200\eta$. Here, $\mathscr{L}$ is the integral length of the longitudinal velocity correlation function. The integral time is $\mathscr{T} = \mathscr{L}/u' \approx 25\tau_\eta$, where u' denotes the r.m.s. value of a component of the velocity, and τ_η is the Kolmogorov time scale.

3.1. *Internal energy and its transfer rate*

The total kinetic energy $K(\boldsymbol{x}, t|\ell)$ per unit mass of fluid particles in the cube $V(\boldsymbol{x}|\ell)$ of size ℓ^3 centred at $\boldsymbol{x}$ is

$$K(\boldsymbol{x}, t|\ell) = \frac{1}{2\,\ell^3} \int_{V(\boldsymbol{x}|\ell)} \left|\boldsymbol{u}(\boldsymbol{x}', t)\right|^2 \mathrm{d}\boldsymbol{x}'. \tag{3.1}$$

We decompose $K(\boldsymbol{x}, t|\ell)$ into the translational energy $E(\boldsymbol{x}, t|\ell)$ and the internal energy $\widetilde{U}(\boldsymbol{x}, t|\ell)$ as

$$E(\boldsymbol{x}, t|\ell) = \tfrac{1}{2} \left| \langle \boldsymbol{u}(\boldsymbol{x}, t) \rangle_\ell \right|^2, \tag{3.2}$$

$$\widetilde{U}(\boldsymbol{x}, t|\ell) = \frac{1}{2\,\ell^3} \int_{V(\boldsymbol{x}|\ell)} \left| \boldsymbol{u}(\boldsymbol{x}', t) - \langle \boldsymbol{u}(\boldsymbol{x}, t) \rangle_\ell \right|^2 \mathrm{d}\boldsymbol{x}'. \tag{3.3}$$

Note that $K = E + \widetilde{U}$. Here,

$$\langle \boldsymbol{u}(\boldsymbol{x}, t) \rangle_\ell = \frac{1}{\ell^3} \int_{V(\boldsymbol{x}|\ell)} \boldsymbol{u}(\boldsymbol{x}', t)\, \mathrm{d}\boldsymbol{x}' \tag{3.4}$$

is the mean velocity, i.e. the sweeping velocity of the cube $V(\boldsymbol{x}|\ell)$.

$\widetilde{U}(\boldsymbol{x}, t|\ell)$ is the energy of the flow structures whose size is smaller than ℓ. For example, $\widetilde{U}$ for $\ell = L_0$, the system size, is the total kinetic energy per unit mass in the frame in which the mean velocity vanishes. Therefore, the internal energy $U(\boldsymbol{x}, t|\ell)$ of the structures of size between ℓ and ℓ/α is defined by

$$U(\boldsymbol{x}, t|\ell) = \widetilde{U}(\boldsymbol{x}, t|\ell) - \frac{1}{V'(\boldsymbol{x}|\ell)} \int_{V'(\boldsymbol{x}|\ell)} \widetilde{U}(\boldsymbol{x}', t|\ell/\alpha)\, \mathrm{d}\boldsymbol{x}'. \tag{3.5}$$

Here, $\int_{V'(\boldsymbol{x}|\ell)} \mathrm{d}\boldsymbol{x}'$ denotes the volume integral over the points $\boldsymbol{x}'$ such that $V(\boldsymbol{x}'|\ell/\alpha) \subset V(\boldsymbol{x}|\ell)$. In the followings, we put $\alpha = 2$.

Next, the temporal evolution of the internal energy is considered. It is important to note that the evolution depends on the frame of reference. For example, it is possible to regard the sweeping of small-scale structures by larger-scale flow as the cascade of energy in an inappropriate frame. Therefore, we consider the rate of change of $\widetilde{U}$ in the frame which moves in the sweeping velocity (3.4). Since the velocity and acceleration of a fluid particle at $\boldsymbol{x}$ in this frame are $\boldsymbol{u}(\boldsymbol{x}, t) - \langle \boldsymbol{u}(\boldsymbol{x}, t) \rangle_\ell$ and $\boldsymbol{a}(\boldsymbol{x}, t)$, respectively, the change in its energy per unit time is $\boldsymbol{a}(\boldsymbol{x}, t) \cdot (\boldsymbol{u}(\boldsymbol{x}, t) - \langle \boldsymbol{u}(\boldsymbol{x}, t) \rangle_\ell)$. Hence, the total energy gain per unit time and mass, in this sweeping frame, inside

$V(\boldsymbol{x}|\ell)$ is

$$\widetilde{T}(\boldsymbol{x},t|\ell)=\frac{1}{\ell^3}\int_{V(\boldsymbol{x}|\ell)}\boldsymbol{a}(\boldsymbol{x}',t)\cdot\left(\boldsymbol{u}(\boldsymbol{x}',t)-\langle\boldsymbol{u}(\boldsymbol{x},t)\rangle_\ell\right)\,\mathrm{d}\boldsymbol{x}'. \tag{3.6}$$

Accordingly, the total gain of internal energy (the energy transfer) of structures of size between ℓ and ℓ/α is

$$T(\boldsymbol{x},t|\ell)=\widetilde{T}(\boldsymbol{x},t|\ell)-\frac{1}{V'(\boldsymbol{x}|\ell)}\int_{V'(\boldsymbol{x}|\ell)}\widetilde{T}(\boldsymbol{x}',t|\ell/\alpha)\,\mathrm{d}\boldsymbol{x}'. \tag{3.7}$$

We emphasise again that both U and T are Galilean invariants. The energy transfer T defined above includes the effects of the viscous and external forces, although these may be negligible in the inertial range. We have confirmed that the following argument is not affected even if we exclude these effects from the definition of T. Note also that the Lagrangian temporal correlation of quantities essentially similar to U for different scales has been investigated by Meneveau & Lund (1994) to verify the scale localness of the energy cascade. Their conclusion is consistent with the following argument.

3.2. *Coherent structures responsible for U and T*

We plot in figure 1(*a*,*c*) the regions where $U(\boldsymbol{x},t|\ell)$ is large for two different scales: a relatively small scale $\ell=8\Delta\approx18\eta\approx0.10\mathscr{L}$, and a relatively large one $\ell=32\Delta\approx74\eta\approx0.43\mathscr{L}$. Many of large-$U$ regions form tubular shapes, though some of them are slightly flattened. On the other hand, iso-surfaces of the coarse-grained squared vorticity (enstrophy), which is obtained by the low-pass filtering of the Fourier modes of vorticity at the cut-off wavenumber $k_c=2\pi/\ell$, are plotted in figure 1(*b*,*d*). Comparing (*b*,*d*) with (*a*,*c*), it is clear that the regions of large U surprisingly coincide with those of large coarse-grained enstrophy. This is also confirmed quantitatively. For $\ell=18\eta$ (or $\ell=74\eta$), at the 77 % (or 75 %) of points where the coarse-grained enstrophy is larger than its mean value, the internal energy is also larger than its mean. Furthermore, for $\ell=18\eta$ (or $\ell=74\eta$), although the points where the coarse-grained enstrophy is larger than its mean occupy only 29 % (or 34 %) of the whole domain, 51 % (or 50 %) of U is confined inside these regions. Hence, we may conclude that internal energy of scale ℓ is possessed mainly by the tubular vortices of the scale.

Next, we plot in figure 2(*a*) the regions (dark-coloured objects) where the negative energy transfer $-T(\boldsymbol{x},t|\ell=74\eta)$ takes large values, together with the iso-surfaces of the coarse-grained enstrophy (light-coloured objects). At this relatively large scale, the regions where the internal energy decreases (i.e. the energy cascades) exist between the coarse-grained vortices. We plot in figure 2(*b*) the regions where the coarse-grained strain $S_{ij}(\boldsymbol{x},t|\ell)$ is large (the iso-surface of coarse-grained total strain, $S_{ij}S_{ij}$) by dark-coloured objects. It is clearly observed that the coarse-grained strain is large between the tubular vortices that are coarse-grained at the same scale. This observation permits us to suggest that the known properties of the (not-coarse-grained) vorticity and strain may be extended to their coarse-grained counterparts. It has been shown (Goto & Kida 2003) that tubular vortices with radii $O(\eta)$ tend to form clusters, especially in an anti-parallel manner, and strong strains perpendicular to such vortex pairs are created between them. These features are likely to be valid for larger vortices than η (see the further discussion in § 4). It is this strong strain, perpendicular to coarse-grained vortices, existing between them that plays a role in the energy cascade. This can be confirmed by comparing figures 2(*a*) and 2(*b*); both regions where the internal energy of size ℓ decreases and where the coarse-grained (at this scale ℓ) strain is large exist between the coarse-grained (at this scale ℓ) tubular vortices, and the spatial

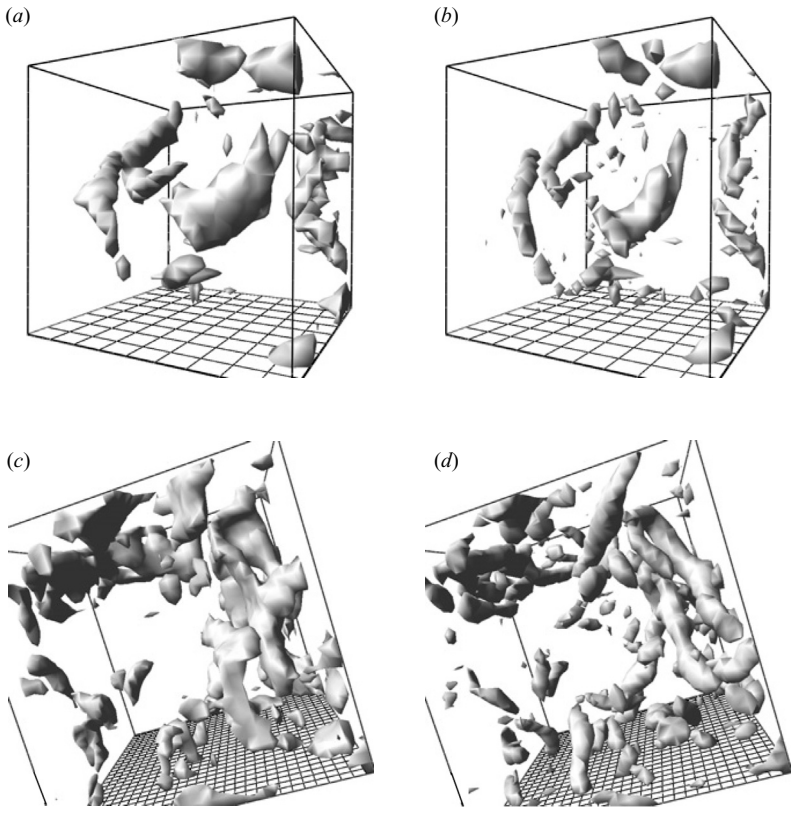

FIGURE 1. (*a*, *c*) Iso-surfaces of internal energy of scale ℓ. (*b*, *d*) Iso-surfaces of enstrophy coarse-grained at ℓ. (*a*, *b*) $\ell = 18\eta$. The size of cube shown is $(1.1\mathscr{L})^3 \approx (190\eta)^3$. Thresholds are set at the mean m plus the standard deviation σ. (*c*, *d*) $\ell = 74\eta$. The size of cube shown is $(3.5\mathscr{L})^3 \approx (600\eta)^3$. Thresholds are set at $m + 1.5\sigma$. Note that, in figures 1–6, the width of the bottom grid is 20η.

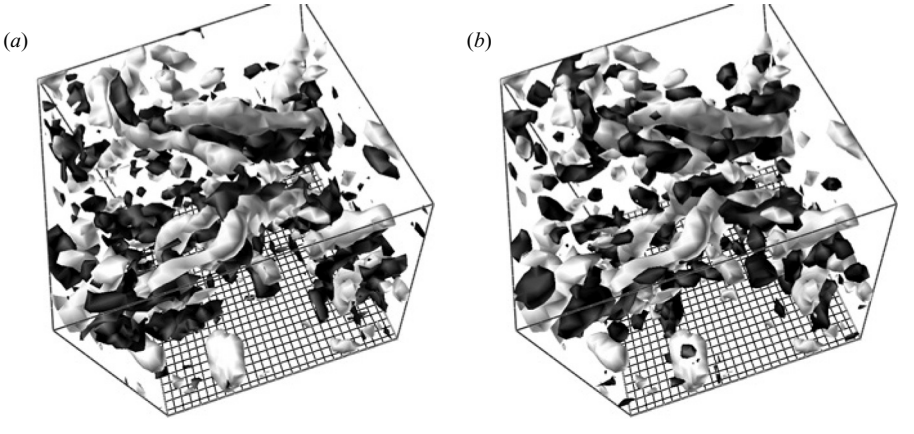

FIGURE 2. (*a*) Iso-surfaces of coarse-grained enstrophy (light-coloured objects) and negative energy transfer (dark-coloured objects) at the scale $\ell = 74\eta$. (*b*) Iso-surfaces of coarse-grained enstrophy (light-coloured objects) and coarse-grained total strain (dark-coloured objects). The thresholds are set at $m + 1.5\sigma$. The size of the cube shown is $(3.5\mathscr{L})^3 \approx (600\eta)^3$.

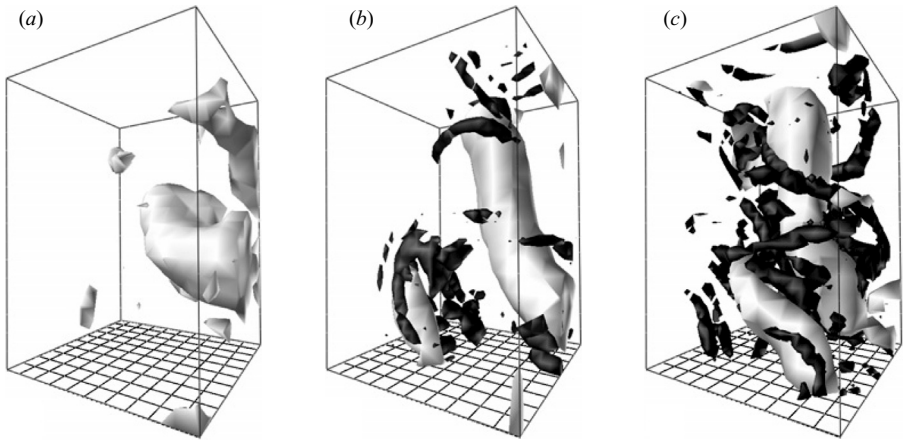

FIGURE 3. An example of the regeneration of small-scale vortices in an initially coarse-grained field. Light-coloured objects are the iso-surfaces of coarse-grained enstrophy at a relatively large scale (74η), whereas dark-coloured objects are those at relatively small scale (18η). The size of the box is $200\eta \times 200\eta \times 300\eta$. (*a*) $t = 0$, (*b*) $13\tau_\eta$ ($0.56\mathscr{T}$) and (*c*) $27\tau_\eta$ ($1.1\mathscr{T}$). See also movie 1, available with the online version, in which we can observe that an anti-parallel pair of large-scale vortices creates smaller-scale vortices between them.

distributions of these two iso-surfaces coincide with each other well, though not perfectly. Quantitatively, for $\ell = 18\eta$ (or 75η), the regions where the coarse-grained total strain takes larger values than its mean occupy only 34 % (or 38 %) of the whole domain, and 67 % (or 58 %) of the negative energy transfer takes place in these regions. Thus, we may conclude that a large amount of the energy cascades takes place in strong (coarse-grained) strain regions between the pairs of tubular (coarse-grained) vortices. Note also that the ratio of 58 % to 38 % is not very large. This may be because strong vortex stretching requires not only a strong strain but also alignment between the vorticity and the strain.

Looking again at figure 1, it is seen that the iso-surfaces of the internal energy are slightly flattened compared to the iso-surfaces of the coarse-grained enstrophy, especially in the regions where many vortices exist. This is because the internal energy inside the coarse-grained vortices transfers to the high-straining regions, and the energy cascades. It is confirmed that the negative energy transfer takes large values in the regions where the internal energy is large but the coarse-grained enstrophy is not large.

In conclusion, since the internal energy of scale ℓ tends to accumulate inside the coarse-grained tubular vortices, the energy cascade from scale ℓ to ℓ' must correspond to the generation of tubular vortices with radii $O(\ell')$ by the vortices with radii $O(\ell)$. Since the regions in which the internal energy of scale ℓ decreases are concentrated in the strong straining regions of scale ℓ, the energy cascade may be regarded as the stretching of smaller-scale vortices in this larger-scale strain field which exists between the pairs of tubular vortices of scale ℓ.

3.3. *Examples of the energy cascade*

In order to observe an example of the energy cascade, we show in figure 3 (and movie 1, available with the online version) the temporal evolution of an artificial field (data B) where flow structures smaller than $L_0/k_c \approx 74\eta$ are removed by low-pass filtering of the Fourier modes of data A. Only large-scale vortices exist initially (figure 3*a*),

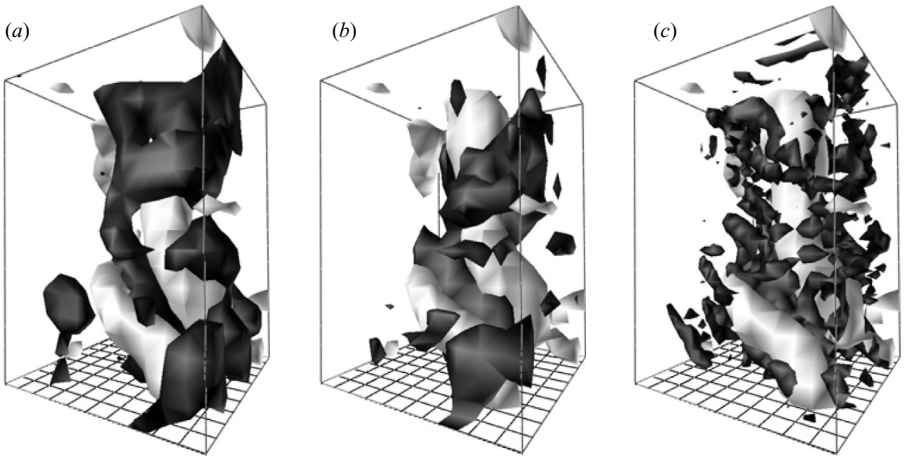

FIGURE 4. Light-coloured objects are the large-scale ($\ell = 74\eta$) vortices at the same time as figure 3(*c*). Dark-coloured objects are the iso-surfaces of: (*a*) the coarse-grained total strain at the large scale $\ell = 74\eta$, (*b*) the negative energy transfer (loss) at $\ell = 74\eta$ and (*c*) the positive energy transfer (gain) at a small scale, $\ell = 18\eta$.

but when two of these vortices (which are anti-parallel with each other) meet, smaller vortices are created between the pair (figure 3*b*,*c*). The smaller-scale vortices created tend to wrap around the larger-scale vortex pair in the direction perpendicular to them. This is because a strong strain field is created between the pair of tubular vortices.

Figure 4(*a*) shows the iso-surface of the total strain at the large scale $\ell = 74\eta$ at the same time as figure 3(*c*). As expected from figure 2, a strong strain field in this scale exists between the anti-parallel vortex pair (the two big light-coloured objects). Figures 4(*b*) and 4(*c*) show the iso-surfaces of the negative energy transfer at the large scale (74η) and of the positive energy transfer at a smaller scale (18η), respectively. It is observed that large-scale structures lose their energy in the strong straining regions observed in figure 4(*a*), whereas smaller-scale structures gain the energy. Note also that the energy which the smaller-scale structures acquire is possessed by strong vortices of the smaller scale (as observed in figures 3*c* and 4*c*).

The next step of the energy cascade can be also observed in figure 5 (and online movie 2), where the iso-surface (dark-coloured objects) of the enstrophy coarse-grained at 18η is plotted together with that (light-coloured objects) at 4.5η. A smaller-scale vortex tube is created in the direction perpendicular to an anti-parallel pair of the larger-scale vortex tubes. Note that the smallest vortex tubes have radii of about 5η (Goto & Kida 2003), and therefore 18η is almost the smallest length scale in this turbulence. Hence, it is relatively rare for these vortices to create smaller ones, overcoming the viscous diffusion.

Because of the moderate Reynolds number of our DNS, it is not possible to capture the energy cascade for more than these two steps. However, the above observations strongly support the scenario that the energy cascade is caused by the stretching of smaller-scale vortices in the large-scale strain field.

It is important to verify that the phenomenon observed in the filtered field (data B) is relevant also in the more realistic statistically stationary field (data A). Similar observations to figure 3 are easily made in the latter field, and an example is given in figure 6 (and online movie 3). When an anti-parallel pair of relatively larger-scale

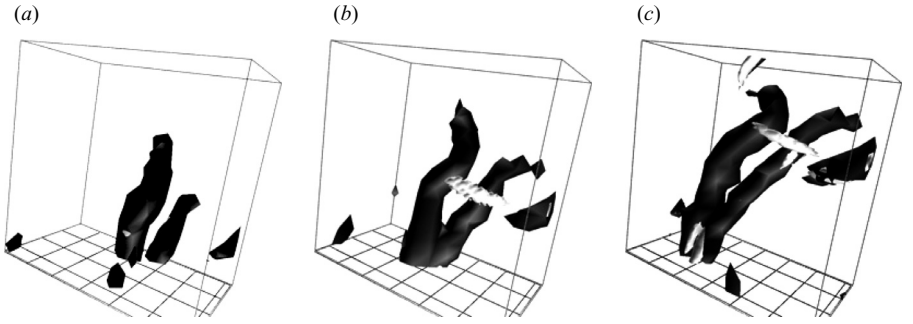

FIGURE 5. The next step of the energy cascade. Dark-coloured objects are the iso-surfaces of coarse-grained enstrophy at 18η (same size as in figures 3 and 4), whereas light-coloured objects are those at a smaller scale 4.5η. The size of the box is $130\eta \times 130\eta \times 74\eta$. (*a*) $t = 21\tau_\eta$, (*b*) $24\tau_\eta$ and (*c*) $27\tau_\eta$. See also online movie 2.

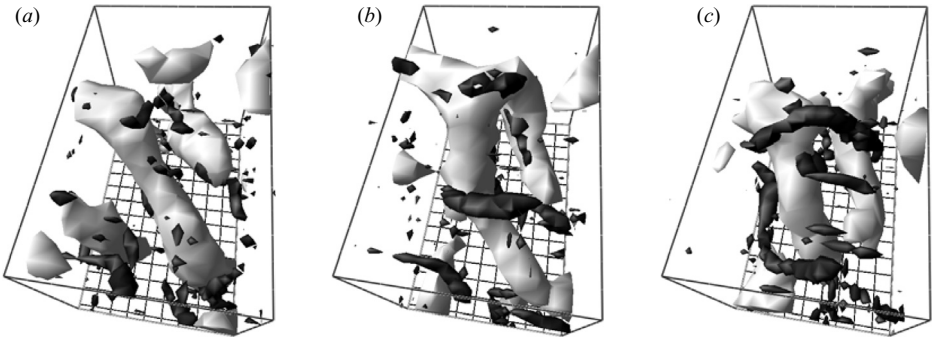

FIGURE 6. Smaller-scale vortex creation by larger-scale vortices in statistically stationary turbulence. Light-coloured objects are the iso-surfaces of coarse-grained enstrophy at a relatively large scale (74η), whereas dark-coloured objects are those at relatively small scale (18η). The size of the box is $180\eta \times 180\eta \times 300\eta$. Time elapses from (*a*) to (*c*) with the increment $6.8\tau_\eta$. See also the online movie 3.

(coarse-grained at 75η) vortex tubes meet (figure 6*a*), smaller-scale (18η) tubes are created between them (figure 6*b*,*c*).

Here, it may be worth mentioning another mechanism of energy cascade. Some authors have noted that the roll-up of vortex sheets plays a role in the cascade. Although rolling up is rarely observed in the above DNS, it may be natural for large-scale vortex sheets to be created between pairs of larger-scale vortices before the creation of smaller-scale tubular vortices (the rolling up could be very fast). In this sense, the scenario based on roll-up is not necessarily inconsistent with the one described in § 2. It is also important to refer to the related study by Melander & Hussain (1993), where the interaction between large-scale coherent tubular vortices and turbulence is investigated, and the creation of small-scale tubular vortices perpendicular to the coherent large-scale ones is found numerically.

3.4. *Spatial intermittency of the energy cascade*

It is ironic that the energy cascade picture, which serves as the basis of the Kolmogorov similarity hypothesis, forces a correction of the hypothesis itself (see Frisch 1995). Because the energy transfer becomes spatially intermittent at smaller scales, and because the degree of the intermittency increases as the scale decreases, we cannot

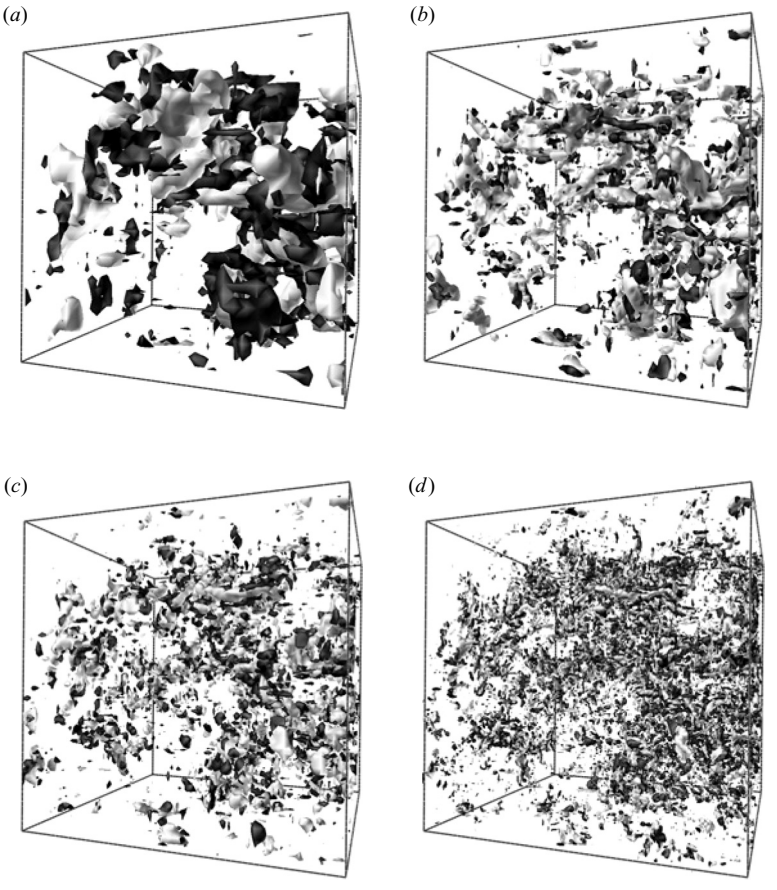

FIGURE 7. Iso-surfaces of the internal energy $U(\boldsymbol{x}, t|\ell)$ (light-coloured objects) and the negative energy transfer rate $-T(\boldsymbol{x}, t|\ell)$ (dark-coloured objects) for four different scales. The box is the entire simulation box: $(7\mathscr{L})^3 \approx (1200\eta)^3$. The thresholds are set as the mean plus s times the standard deviations: (*a*) $\ell = 150\eta$, $s = 1.5$. (*b*) $\ell = 74\eta$, $s = 2$. (*c*) $\ell = 37\eta$, $s = 2.5$. (*d*) $\ell = 18\eta$, $s = 3$.

describe accurately the statistics of turbulence at small scales only using the mean value of the energy transfer rate. This intermittent property of energy transfer (and the energy dissipation) has been confirmed by laboratory experiments (Batchelor & Townsend 1949; see also Bandi *et al.* 2006 for a recent development) and by DNS (She, Jackson & Orszag 1991). Many physical models of the energy cascade (for example, the β model by Frisch, Sulem & Nelkin 1978 and its descendants) explain the spatial intermittency of the energy transfer, and of the energy dissipation. It can be confirmed that the view of these cascade models is consistent with the scenario described in § 2.

Figure 7 shows the regions of large internal energy (light-coloured objects) and large negative energy transfer (dark-coloured ones) for four different scales. As is well known, active regions at smaller scales are localized more intermittently. It is also observed that the small-scale active regions exist only near to the regions where large-scale motions are energetic. This is consistent with the scenario described in § 2; since the energy cascade is due to the creation of smaller-scale vortices in strong straining regions between vortex pairs at larger scales, the energy transfer becomes

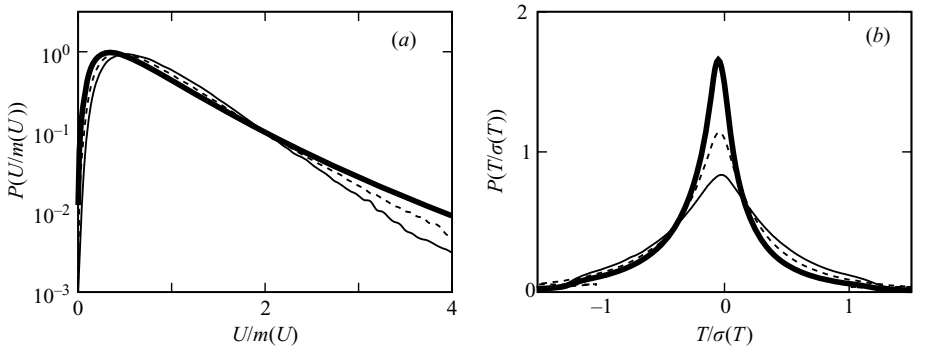

FIGURE 8. PDF of (*a*) $U(\boldsymbol{x}, t|\ell)$ and (*b*) $T(\boldsymbol{x}, t|\ell)$ for three different ℓ. Here, m and σ denote the mean and the standard deviation, respectively. Thin solid curve, $\ell = 74\eta$; thin broken curve, 37η; thick solid curve, 18η. Averaged over 80 snapshots.

more localized in space at smaller scales. This feature is confirmed quantitatively in figure 8 where the probability density functions (PDF) of U and T are plotted for three different ℓ. It is observed that the tail of $P(U)$ is broader and the kurtosis of $P(T)$ is larger for smaller scales.

Note also, in passing, that the regions in which U for smaller scales concentrates tend to exist between the regions in which U for larger scales concentrates, and therefore smaller-scale vortices exist between the pairs of larger-scale vortices rather than inside them. Hence, it is not generally appropriate to regard a large-scale vortex as the cluster of smaller-scale vortices.

4. Concluding remarks

It is shown that the energy cascade in homogeneous isotropic turbulence can be caused by the process whereby tubular vortex pairs stretch smaller-scale vortices. Examples of this scenario (§ 2) are numerically demonstrated in figures 3–6 (and moves 1–3, online), although only the first two steps of the energy cascade can be captured by our DNS due to the smallness of the Reynolds number ($R_\lambda \approx 187$). Analyses of higher-Reynolds-number flows are desirable to further verify the scenario.

Here, we note that all of the parent vortex pairs observed in these examples (figures 3–6) are anti-parallel with each other. Anti-parallel vortex pairs are likely to play a role in the energy cascade because such pairs create strong strains between them, and because the majority of the energy transfer takes place in strong strains between vortex pairs as shown in § 3.2. However, there is no quantitative support of the role of anti-parallel vortex pairs, and this is an important problem for the future. The physical mechanism of formation of anti-parallel vortex pairs is also unknown. There are at least two possibilities. One is that, as observed in Melander & Hussain (1993), a larger vortex tube creates anti-parallel pairs of smaller vortex tubes around it. The other is that Siggia's (1985) mechanism makes a vortex tube align with another tube in an anti-parallel manner.

It must be also mentioned that scenarios of the energy cascade based on vortex stretching have been strongly questioned by Tsinober (2001) because the vortex stretching cannot play a direct role in the creation of strong straining regions, where the final stage (the energy dissipation) takes place. However this is not necessarily a rebuttal of the scenario described in § 2, since the energy dissipation (and transfer)

takes place between pairs of vortices. This implies that the vortex stretching plays an indirect role in the energy cascade.

Before closing this article, we discuss the localness of this process in scale. According to the Kolmogorov scaling, a typical swirling velocity of the vortices with radii $O(\ell)$ may be $\epsilon^{1/3}\ell^{1/3}$. (Here, ϵ is the mean energy dissipation rate per unit mass.) Therefore, when two vortices of this scale meet, the strain rate between the pair becomes the order of $\epsilon^{1/3}\ell^{-2/3}$. Let the radius of the next generation of tubular vortices created by this strain be ℓ'. If the strain keeps stretching the smaller-scale vortices until the strain balances the viscous diffusion in the sense of the Burgers vortex tube, ℓ' can be as small as

$$\ell'_{\min} \sim \sqrt{\nu/(\epsilon^{1/3}\ell^{-2/3})} \sim \ell\, Re^{-1/2}\,(\mathscr{L}/\ell)^{2/3}. \tag{4.1}$$

Here, $Re \sim u'\mathscr{L}/\nu$ is the Reynolds number. However, since the smaller vortices are likely to escape out of the strong strain region before its radius decreases to $\ell'_{\min}$, ℓ' is generally larger than $\ell'_{\min}$. Incidentally, $\ell'_{\min}$ becomes η for $\ell = \eta$. This implies that the Kolmogorov-scale vortices cannot create smaller ones. On the other hand, for $\ell = \mathscr{L}$ (the integral length), $\ell'_{\min} \sim \mathscr{L}Re^{-1/2}$, i.e. the Taylor length λ. This implies that tubular vortices with radii $O(\mathscr{L})$ cannot create vortices smaller than λ. It is important that the largest vortices of size $\mathscr{L}$ cannot directly create the smallest flow structures of size η. In this sense, the scale localness of the energy cascade might be assured. However, if a rapid cascade such as the one from $\mathscr{L}$ to λ successively takes place n times, very fine structures of size

$$\ell_n \sim \mathscr{L}\, Re^{-3(1-(1/3)^n)/4} \tag{4.2}$$

are created rapidly. If such a rapid cascade is ubiquitous, the small-scale universality may be questionable. Since our method cannot verify the localness of the energy cascade quantitatively, another method to define the scale-to-scale energy transfer, by wavelet functions for example, is needed for further discussions.

The author would like to thank Professors J. C. Vassilicos and S. Kida for their valuable comments on a draft of the present article. The DNS was carried out on NEC SX-7/160M5 with the support of the NIFS Collaborative Program.

REFERENCES

Bandi, M. M., Goldburg, W. I., Cressman, Jr., J. R. & Pumir, A. 2006 Energy flux fluctuations in a finite volume of turbulent flow. *Phys. Rev.* E **73**, 026308.

Batchelor, G. K. & Townsend, A. A. 1949 The nature of turbulent motion at large wavenumbers. *Proc. R. Soc. Lond.* A **199**, 238–255.

Brachet, M. E. 1991 Direct simulation of three-dimensional turbulence in the Taylor-Green vortex. *Fluid Dyn. Res.* **8**, 1–8.

Chen, S., Ecke, R. E., Eyink, G. L., Rivera, M., Wan, M. & Xiao, Z. 2006 Physical mechanism of the two-dimensional inverse energy cascade. *Phys. Rev. Lett.* **96**, 084502.

Davidson, P. A. 2004 *Turbulence: An Introduction for Scientists and Engineers*. Oxford University Press.

Domaradzki, J. A. & Rogallo, R. S. 1990 Local energy transfer and nonlocal interactions in homogeneous, isotropic turbulence. *Phys. Fluids* A **2**, 413–426.

Eyink, G. L. 2005 Locality of turbulent cascade. *Physica* D **207**, 91–116.

Farge, M. 1992 Wavelet transforms and their applications to turbulence. *Annu. Rev. Fluid Mech.* **24**, 395–457.

Frisch, U. 1995 *Turbulence, The Legacy of A. N. Kolmogorov*. Cambridge University Press.

Frisch, U., Sulem, P. L. & Nelkin, M. 1978 A simple dynamical model of intermittent fully developed turbulence. *J. Fluid Mech.* **87**, 719–736.

Goto, S. & Kida, S. 2003 Enhanced stretching of material lines by antiparallel vortex pairs in turbulence. *Fluid Dyn. Res.* **33**, 403–431.

Hunt, J., Sandham, N., Vassilicos, J., Launder, B., Monkewitz, P. & Hewitt, G. 2001 Development in turbulence research: a review based on the 1999 program of the Isaac Newton Institute, Cambridge. *J. Fluid Mech.* **436**, 353–391.

Jiménez, J., Wray, A. A., Saffman, P. G. & Rogallo, R. S. 1993 The structure of intense vorticity in isotropic turbulence. *J. Fluid Mech.* **255**, 65–90.

Kerr, R. M. 1985 Higher-order derivative correlations and the alignment of small-scale structures in isotropic numerical turbulence. *J. Fluid Mech.* **153**, 31–58.

Kida, S. & Miura, H. 2000 Double spirals around a tubular vortex in turbulence. *J. Phys. Soc. Japan* **69**, 3466–3467.

Kolmogorov, A. N. 1941 The local structure of turbulence in incompressible viscous fluid for very large Reynolds numbers. *Dokl. Akad. Nauk SSSR* **30**, 301–305, English translation in *Proc. R. Soc. Lond.* A **434**, 9–13 (1991).

Kraichnan, R. H. 1965 Lagrangian-history closure approximation for turbulence. *Phys. Fluids* **8**, 575–598 (erratum **9**, *ibid.,* 1884).

Kraichnan, R. H. 1971 Inertial-range transfer in two- and three-dimensional turbulence. *J. Fluid Mech.* **47**, 525–535.

Melander, M. & Hussain, F. 1993 Coupling between a coherent structure and fine-scale turbulence. *Phys. Rev.* E **48**, 2669–2689.

Meneveau, C. & Lund, T. S. 1994 On the Lagrangian nature of the turbulence energy cascade. *Phys. Fluids* **6**, 2820–2825.

Ohkitani, K. & Kida, S. 1992 Triad interactions in a forced turbulence. *Phys. Fluids* A **4**, 794–802.

Pumir, A., Shraiman, B. I. & Chertkov, M. 2001 The Lagrangian view of energy transfer in turbulent flow. *Europhys. Lett.* **56**, 379–385.

Richardson, L. F. 1922 *Weather Prediction by Numerical Process*. Cambridge University Press.

She, Z. S., Jackson, E. & Orszag, S. A. 1991 Structure and dynamics of homogeneous turbulence - models and simulations. *Proc. Roy. Soc. Lond.* A **434**, 101–124.

Siggia, E. D. 1985 Collapse and amplification of a vortex filament. *Phys. Fluids* **28**, 794–805.

Tsinober, A. 2001 *An Informal Introduction to Turbulence*. Kluwer.

Vincent, A. & Meneguzzi, M. 1994 The dynamics of vorticity in homogeneous turbulence. *J. Fliud Mech.* **258**, 245–254.

Yeung, P. K. & Brasseur, J. G. 1991 The response of isotropic turbulence to isotropic and anisotropic forcing at large scales. *Phys. Fluids* A **3**, 884–897.